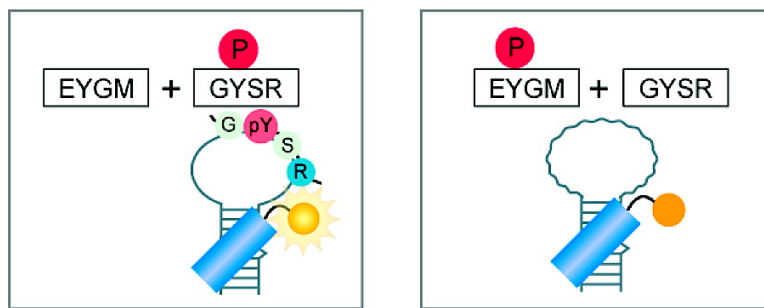Article

Context-Dependent Fluorescence Detection of a Phosphorylated Tyrosine Residue by a Ribonucleopeptide

Tetsuya Hasegawa, Masaki Hagihara, Masatora Fukuda,
Shun Nakano, Nobutaka Fujieda, and Takashi Morii

More About This Article

Additional resources and features associated with this article are available within the HTML version:

- Supporting Information
- Access to high resolution figures
- Links to articles and content related to this article
- Copyright permission to reproduce figures and/or text from this article

View the Full Text HTML

Context-Dependent Fluorescence Detection of a Phosphorylated Tyrosine Residue by a Ribonucleopeptide

Tetsuya Hasegawa,[†] Masaki Hagihara,[‡] Masatora Fukuda,[‡] Shun Nakano,[‡] Nobutaka Fujieda,[§] and Takashi Morii*,[†,‡]

Institute of Advanced Energy, Institute of Sustainability Science, and Pioneering Research Unit for Next Generation, Kyoto University, Uji, Kyoto 611-0011, Japan

Received March 8, 2008; Revised Manuscript Received April 21, 2008; E-mail: t-morii@iae.kyoto-u.ac.jp

Abstract: Tools for selective recognition and sensing of specific phosphorylated tyrosine residues on the protein surface are essential for understanding signal transduction cascades in the cell. A stable complex of RNA and peptide, a ribonucleopeptide (RNP), provides effective approaches to tailor RNP receptors and fluorescent RNP sensors for small molecules. In vitro selection of an RNA-derived pool of RNP afforded RNP receptors specific for a phosphotyrosine residue within a defined amino-acid sequence Gly-Tyr-Ser-Arg. The RNP receptor for the specific phosphotyrosine residue was successfully converted to a fluorescent RNP sensor for sequence-specific recognition of a phosphorylated tyrosine by screening a pool of fluorescent phosphotyrosine-binding RNPs generated by a combination of the RNA subunits of phosphotyrosine-binding RNPs and various fluorophore-modified peptide subunits. The phosphotyrosine-binding RNP receptor and fluorescent RNP sensor constructed from the RNP receptor not only discriminated phosphotyrosine against tyrosine, phosphoserine, or phosphothreonine, but also showed specific recognition of amino acid residues surrounding the phosphotyrosine residue. A fluorescent RNP sensor for one of the tyrosine phosphorylation sites of p100 coactivator showed a binding affinity to the target site 95-fold higher than the other tyrosine phosphorylation site. The fluorescent RNP sensor has an ability to function as a specific fluorescent sensor for the phosphorylated tyrosine residue within a defined amino-acid sequence in HeLa cell extracts.

Introduction

A reversible and dynamic process of protein phosphorylation regulated by protein kinases and phosphatases is one of the most common post-translational protein modifications to regulate protein activity in nearly every aspect of eukaryotic cell biology.[1] Phosphorylation of tyrosine residues within specific amino acid sequences is found in a large number of proteins that mediate signal transduction pathways.[2,3] The distribution of amino acid residues surrounding phosphotyrosine is distinct for each cell line and likely reflects the substrate recognition motifs of the underlying activated protein kinases. The specificity of protein kinase is determined by acidic, basic, or hydrophobic residues adjacent to the phosphorylated residue.[4] Recently, more than 600 distinct tyrosine phosphorylation sites have been reported in mammalian proteome.[5] Furthermore, a single protein is phosphorylated and dephosphorylated by different tyrosine kinases and phosphatases, respectively, on a different site at a specific occasion. Such a large variation makes it difficult to manually inspect the phosphorylated protein sequences and to predict the location of biologically active phosphorylation sites.

Identification of the specific tyrosine phosphorylation sites is an essential step to understand the role of phosphorylation for a given biochemical function. A number of techniques have been used to detect phosphoproteins, such as radiolabeling,[6] antibody recognition,[7] and mass spectrometry.[5,8] Among these, antibodies that recognize specific phosphopeptides have been the most specific affinity probes to differentiate phosphorylated and nonphosphorylated states of proteins. These antibodies have been widely used to assess tyrosine phosphorylation of a number of proteins, but it is difficult to obtain quantitative interpretation due to the washing steps involved in the analytical procedures, such as immunoblotting techniques. A large number of phosphorylation state-specific antibodies could be utilized to detect a wide variety of proteins. However, production of antibodies is considerably time-consuming, and it is difficult to develop a series of antibodies that reveal similar binding properties. Thus, quantification of protein phosphorylation at a specific tyrosine

---

[†] Institute of Sustainability Science.
[‡] Institute of Advanced Energy.
[§] Pioneering Research Unit for Next Generation.

(1) Johnson, L. N.; Lewis, R. J. *Chem. Rev.* **2001**, *101*, 2209–2242.
(2) Jackson, M. D.; Denu, J. M. *Chem. Rev.* **2001**, *101*, 2313–2340.
(3) Chen, Z.; Gibson, T. B.; Robinson, F.; Silvestro, L.; Pearson, G.; Bing-e, Xu.; Wright, A.; Vanderbilt, C.; Cobb, M. H. *Chem. Rev.* **2001**, *101*, 2449–2476.
(4) Blom, N.; Gammeltoft, S.; Brunak, S. *J. Mol. Biol.* **1999**, *294*, 1351–1362.
(5) Rush, J.; Moritz, A.; Lee, K. A.; Guo, A.; Goss, V. L.; Spek, E. J.; Zhang, H.; Zha, X. M.; Polakiewicz, R. D.; Comb, M. J. *Nat. Biotechnol.* **2005**, *23*, 94–101.

(6) Soling, H. D.; Fest, W.; Schmidt, T.; Esselmann, H.; Bachmann, V. *J. Biol. Chem.* **1989**, *264*, 10643–10648.
(7) Gullick, W. J.; Downward, J.; Waterfield, M. D. *EMBO J.* **1985**, *4*, 2869–2877.
(8) (a) Zhou, H. L.; Watts, J. D.; Aebersold, R. *Nat. Biotechnol.* **2001**, *19*, 375–378. (b) Mann, M.; Ong, S. E.; Gronborg, M.; Steen, H.; Jensen, O. N.; Pandey, A. *Trends Biotechnol.* **2002**, *20*, 261–268. (c) Salomon, A. R.; Ficarro, S. B.; Brill, L. M.; Brinker, A.; Phung, Q. T.; Ericson, C.; Sauer, K.; Brock, A.; Horn, D. M.; Schultz, P. G.; Peters, E. C. *Proc. Natl. Acad. Sci. U. S. A.* **2003**, *100*, 443–448.

---

residue is still a very challenging task, even though antiphosphotyrosine antibodies are available for nearly 80 tyrosine phosphorylation sites.[9] The development of new probes to replace antibodies is necessary to assess the phosphorylation status of proteins such as reagentless biosensors.

Fluorescent biosensors directly transduce binding events into optical signals. Macromolecular or synthetic receptors are modified with fluorophores to transduce ligand binding into measurable optical signals.[10,11] Several artificial receptors for tyrosine phosphorylated peptides or *O*-phospho-L-tyrosine (pY) have been reported. An artificial pY sensor based on β-cyclodextrin modified with ammonium or guanidinium groups showed a dissociation constant of 2.8 mM for pY, which is far less than the affinity needed to practically detect the tyrosine phosphorylation of proteins.[12] A Zn(II) complex of anthracene bisdipicolylamine Zn(II)-Dpa bound and fluorescently responded to a pY residue in a glutamic acid-rich peptide with a dissociation constant of 10^{-7} M.[13] Zn(II)-Dpa could discriminate pY from unmodified tyrosine, but the zinc complex hardly differentiated the pY residues in different surrounding amino acid sequences to detect a specific pY site. Also, the presence of other phosphate-containing molecules, such as ATP or ADP, caused inhibitory effects.

 (9) Mandell, J. W. *Am. J. Pathol.* **2003**, *163*, 1687–1698.
(10) (a) Pollack, S. J.; Nakayama, G. R.; Schultz, P. G. *Science* **1988**, *242*, 1038–1040. (b) Gilardi, G.; Zhou, L. Q.; Hibbert, L.; Cass, A. E. *Anal. Chem.* **1994**, *66*, 3840–3847. (c) Marvin, J. S.; Corcoran, E. E.; Hattangadi, N. A.; Zhang, J. V.; Gere, S. A.; Hellinga, H. W. *Proc. Natl. Acad. Sci. U. S. A.* **1997**, *94*, 4366–4371. (d) Hamachi, I.; Nagase, T.; Shinkai, S. *J. Am. Chem. Soc.* **2000**, *122*, 12065–12066. (e) Benson, D. E.; Conrad, D. W.; de Lorimier, R. M.; Trammell, S. A.; Hellinga, H. W. *Science* **2001**, *293*, 1641–1644. (f) de Lorimier, R. M.; Smith, J. J.; Dwyer, M. A.; Looger, L. L.; Sali, K. M.; Paavola, C. D.; Rizk, S. S.; Sadigov, S.; Conrad, D. W.; Loew, L.; Hellinga, H. W. *Protein Sci.* **2002**, *11*, 2655–2675. (g) Renard, M.; Belkadi, L.; Hugo, N.; England, P.; Altschuh, D.; Bedouelle, H. *J. Mol. Biol.* **2002**, *318*, 429–442. (h) Morii, T.; Sugimoto, K.; Makino, K.; Otsuka, M.; Imoto, K.; Mori, Y. *J. Am. Chem. Soc.* **2002**, *124*, 1138–1139. (i) Toutchkine, A.; Kraynov, V.; Hahn, K. *J. Am. Chem. Soc.* **2003**, *125*, 4132–4145. (j) Chan, P. H.; Liu, H. B.; Chen, Y. W.; Chan, K. C.; Tsang, C. W.; Leung, Y. C.; Wong, K. Y. *J. Am. Chem. Soc.* **2004**, *126*, 4074–4075. (k) Nalbant, P.; Hodgson, L.; Kraynov, V.; Toutchkine, A.; Hahn, K. M. *Science* **2004**, *305*, 1615–1619. (l) Cohen, B. E.; Pralle, A.; Yao, X.; Swaminath, G.; Gandhi, C. S.; Jan, Y. N.; Kobilka, B. K.; Isacoff, E. Y.; Jan, L. Y. *Proc. Natl. Acad. Sci. U. S. A.* **2005**, *102*, 965–970.
(11) (a) Jayasena, S. D. *Clin. Chem.* **1999**, *45*, 1628–1650. (b) Llano-Sotelo, B.; Chow, C. S. *Bioorg. Med. Chem. Lett.* **1999**, *9*, 213–216. (c) Jhaveri, S.; Rajendran, M.; Ellington, A. D. *Nat. Biotechnol.* **2000**, *18*, 1293–1297. (d) Stojanovic, M. N.; de Prada, P.; Landry, D. W. *J. Am. Chem. Soc.* **2000**, *122*, 11547–11548. (e) Jhaveri, S. D.; Kirby, R.; Conrad, R.; Maglott, E. J.; Bowser, M.; Kennedy, R. T.; Glick, G.; Ellington, A. D. *J. Am. Chem. Soc.* **2000**, *122*, 2469–2473. (f) Stojanovic, M. N.; de Prada, P.; Landry, D. W. *J. Am. Chem. Soc.* **2001**, *123*, 4928–4931. (g) Fang, X. H.; Cao, Z. H.; Beck, T.; Tan, W. *Anal. Chem.* **2001**, *73*, 5752–5257. (h) Stojanovic, M. N.; Landry, D. W. *J. Am. Chem. Soc.* **2002**, *124*, 9678–9679. (i) Nutiu, R.; Li, Y. *J. Am. Chem. Soc.* **2003**, *125*, 4771–4778. (j) Stojanovic, M. N.; Green, E. G.; Semova, S.; Nikic, D. B.; Landry, D. W. *J. Am. Chem. Soc.* **2003**, *125*, 6085–6089. (k) Stojanovic, M. N.; Kolpashchikov, D. M. *J. Am. Chem. Soc.* **2004**, *126*, 9266–9270. (l) Yamana, K.; Ohtani, Y.; Nakano, H.; Saito, I. *Bioorg. Med. Chem. Lett.* **2003**, *13*, 3429–3431. (m) Ho, H. A.; Leclerc, M. *J. Am. Chem. Soc.* **2004**, *126*, 1384–1387. (n) Kirby, R.; Cho, E. J.; Gehrke, B.; Bayer, T.; Park, Y. S.; Neikirk, D. P.; McDevitt, J. T.; Ellington, A. D. *Anal. Chem.* **2004**, *76*, 4066–4075. (o) Savran, C. A.; Knudsen, S. M.; Ellington, A. D.; Manalis, S. R. *Anal. Chem.* **2004**, *76*, 3194–3198. (p) Jiang, Y. X.; Fang, X. H.; Bai, C. L. *Anal. Chem.* **2004**, *76*, 5230–5235. (q) Nutiu, R.; Li, Y. *Angew. Chem., Int. Ed.* **2005**, *44*, 1061–1065. (r) Merino, E. J.; Weeks, K. M. *J. Am. Chem. Soc.* **2006**, *127*, 12766–12767.
(12) Cotner, E. S.; Smith, P. J. *J. Org. Chem.* **1998**, *63*, 1737–1739.
(13) (a) Ojida, A.; Mito-oka, Y.; Inoue, M.; Hamachi, I. *J. Am. Chem. Soc.* **2002**, *124*, 6256–6258. (b) Ojida, A.; Mito-oka, Y.; Sada, K.; Hamachi, I. *J. Am. Chem. Soc.* **2004**, *126*, 2454–2463.

Oligonucleotide aptamers obtained by SELEX (systematic evolution of ligands by exponential enrichment) are macromolecular receptors with appropriate affinity and specificity for various targets ranging from small molecules to proteins or even cell membranes.[14] Although the RNA or DNA aptamers are suitable for the structural scaffold of biosensors, no example of a biosensor for targeting a phosphorylated tyrosine residue within a defined amino-acid sequence has been reported. We have previously reported novel methods for constructing ribonucleopeptide (RNP) receptors[15,16] and fluorescent sensors for ATP.[17] A stable RNP scaffold was designed based on the structure of RRE (*R*ev *R*esponsive *E*lement) RNA and Rev peptide complex.[18] The RNA subunit of RNP was utilized to construct an RNA-based library of RNP, from which ATP-binding RNPs were selected by in vitro selection.[14] Subsequent modification of the Rev peptide subunit with a fluorophore enabled us to form a stable fluorescent RNP complex that exerted the fluorescent spectral change upon binding to ATP.[17] Combination of various fluorophore-linked Rev peptides and the RNA subunits of ATP-binding RNP generated fluorescent ATP-binding RNP libraries, which afforded fluorescent ATP sensors with a wide variety of affinities and emission properties, using a simple screening scheme without knowledge of the detailed three-dimensional structure.[17]

RNP receptors targeting pY have been isolated from a pool of RNP that preferentially bound pY over *O*-phospho-L-serine or tyrosine.[19] Though the affinity of pY-binding RNP was a moderate one, the RNP receptor showed a promising selectivity for the phosphorylated tyrosine residue. RNP receptors could target a defined pY-containing amino-acid sequence by expanding the recognition surface within the ligand-binding pocket of RNP. We herein report RNP receptors for a phosphorylated tyrosine-containing tetra-amino-acid sequence Gly-pTyr-Ser-Arg (GpYSR) that shows affinity and specificity much higher than the previous pY-binding RNP receptors. The GpYSR-binding RNP receptor was successfully converted to a fluorescent sensor by a modular strategy using the RNP receptor[17] to detect the tyrosine-phosphorylation at the specific tetra-amino-acid sequence GpYSR (Figure 1), and discriminated the phosphorylated tyrosine residue at the GpYSR sequence against that at the other tyrosine-phosphorylation sequence within the same protein.

Results and Discussion

In Vitro Selection of RNP Receptors for a Phosphorylated Tyrosine-Containing Tetra-Amino-Acid Motif. Phosphoproteins usually contain one or more phosphorylated sites (P-sites) recognized by kinases and phosphatases. A number of tri- or tetra-amino-acid motifs containing phosphorylated tyrosine

(14) (a) Ellington, A. D.; Szostak, J. W. *Nature* **1990**, *346*, 818–822. (b) Tuerk, C.; Gold, L. *Science* **1990**, *249*, 505–510. (c) Breaker, R. R. *Chem. Rev.* **1997**, *97*, 371–390. (d) Osborne, S. E.; Ellington, A. D. *Chem. Rev.* **1997**, *97*, 349–370. (e) Wilson, D. S.; Szostak, J. W. *Annu. Rev. Biochem.* **1999**, *68*, 611–647. (f) Joyce, G. F. *Annu. Rev. Biochem.* **2004**, *73*, 791–836.
(15) Morii, T.; Hagihara, M.; Sato, S.; Makino, K. *J. Am. Chem. Soc.* **2002**, *124*, 4617–4622.
(16) Sato, S.; Fukuda, M.; Hagihara, M.; Tanabe, Y.; Ohkubo, K.; Morii, T. *J. Am. Chem. Soc.* **2005**, *127*, 30–31.
(17) Hagihara, M.; Fukuda, M.; Hasegawa, T.; Morii, T. *J. Am. Chem. Soc.* **2006**, *128*, 12932–12940.
(18) Battiste, J. L.; Mao, H.; Rao, N. S.; Tan, R.; Muhandiram, D. R.; Kay, L. E.; Frankel, A. D.; Williamson, J. R. *Science* **1996**, *273*, 1547–1551.
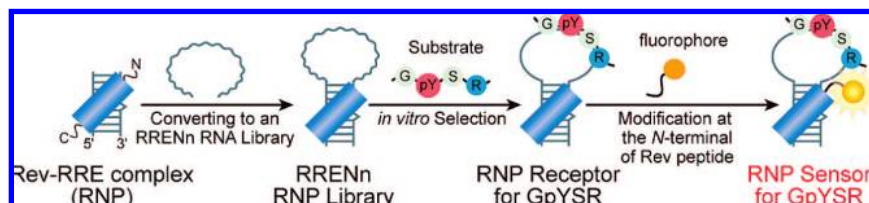(19) Hasegawa, T.; Ohkubo, K.; Yoshikawa, S.; Morii, T. *J. Surf. Sci. Nanotech.* **2005**, *3*, 33–37.

Figure 1. Strategy to obtain RNP fluorescent sensors specific for a phosphotyrosine-containing amino acid sequence GpYSR. Combination of the RNA subunit of the GpYSR-binding RNP and a fluorophore-modified Rev peptide provided a GpYSR RNP fluorescent sensor.

clone	nucleotide sequences of the randomized region	nucleotide lengths
RNA20	UACUUAAGUCGCGCG**GU AUCAG** AUCAC **GAG** AACGCAAC	37nt
RNA19	UGC**GA AUCAG** UUCGG **GAG** GACAUGCGAGAAUUGU	34nt
RNA35	UA **AACAG** AGCU **GCG** CAUUAAUUACACA	27nt
RNA34	CGA **AUCAG** AUCGC **GAG** GA	18nt
RNA33	AUGA **AUCAG** AGCGC **GAG** GGU	20nt
RNA17	GGU **AUCAG** AUCAA **GAG** AGUGCGUCCUGCUAAUG	33nt
RNA28	CUUUUCUGA **AUCAG** AUCGC **GAG** GUGUAUUUG	31nt
RNA05	AUUUCGC**GA AUCAG** GUCGG **GAG** GACGAUGA	30nt
RNA37	GUGGU **AUCAG** AUCGG **GAG** AGGG	22nt
RNA26	GGU **AUCAG** AUCGG **GAG** AG	18nt
RNA38	GC**GA AUCAG** AGCGC **GAG** GAU	20nt
RNA42	UGC**GA AUCAG** AGCGC **GAG** GAU	21nt
RNA36	AUGCCGCCAGUUUUGUCACGA	20nt

Figure 2. Nucleotide sequences obtained for the randomized region of RRENn of GpYSR-binding RNP receptors show consensus sequences (bold).

residues have been identified. To test whether the RNP receptor could discriminate tetra-amino-acid motifs within the same protein, we have focused on tetra-amino-acid motifs EYGM and GYSR corresponding to Y88 and Y883, respectively, of p100 coactivator.[5] The coactivator p100 was originally characterized as a transcriptional coactivator for Epstein−Barr virus nuclear antigen 2 (EBNA-2), which activates transcription of specific genes and is essential for B-lymphocyte transformation.[20] Y883-phosphorylated or Y88-phosphorylated peptides, originated from p100 coactivator, were detected in the fraction of pervanadate-trypsin-treated Jurkat cell or trypsin-treated SU-DHL1 cancer cells.[5] Because each P-site, GYSR and EYGM, contains basic or acidic amino acid residues, respectively, these two P-sites within the same protein would serve as appropriate cases for demonstrating the selectivity of RNP receptors.

From an RNP library generated by randomized 30 nucleotides (RREN30), we have previously isolated RNP receptors with a moderate affinity for *O*-phospho-L-tyrosine.[19] In the RNP structure, active sites within the RNP receptor are stabilized by a complex formation of the Rev peptide and the RRE RNA. At the same time, the complex formation between Rev and RRE would constrain conformational variations of active sites within the randomized nucleotide region of a fixed nucleotide length. Because the active site of RNA aptamers are usually composed from 20 to 40 nucleotides,[21] we have generated an RNP library consisting of various lengths of randomized nucleotides, instead of the randomized nucleotides with fixed lengths, to isolate RNP receptors for a phosphorylated tyrosine residue in a defined amino acid sequence GYSR.

An RNA library RRENn consisted of the RRE region as the Rev peptide binding site and a randomized region containing up to 40 nucleotides adjacent to the RRE region. Chemically synthesized top-strand DNA containing randomized 40 nucleotides was capped with 3′-phosphate group. Annealing the top-strand DNA with bottom-strand DNA containing randomized 7 nucleotides and successive Klenow polymerase reaction and PCR amplification provided double-stranded DNA templates containing 2 to 39 randomized nucleotides between the RRE regions, as confirmed by the sequencing analysis of the initial pool (Figure S1 of the Supporting Information). The RRENn DNA templates were transcribed, and the resulting RRENn RNA pool was followed by adding the Rev peptide to afford RRENn based RNP library. The diversity of RRENn RNP library ($\sim 10^{24}$) is much greater than that of the RREN20 RNP library[15] or RREN30 RNP library[16,17,19] used in our previous study. The present RNP library with a variety of nucleotide lengths would permit more favorable conformational freedom to arrange an active site with a high affinity to a ligand than the previous RNP libraries.

The RNP receptors for the phosphotyrosine-containing GpYSR peptide were obtained by passing a random RRENn RNP pool over a column of immobilized targeted peptide, washing away unbound RNP species, and then eluting the bound RNP with a free GpYSR peptide. After 12 cycles of selection and amplification, the pool of RNP revealed an enhanced GpYSR-binding activity. Cloning and sequencing of selected RNP revealed convergent sequences within 18 to 37 nucleotides that were derived from the randomized RNA region (Figure 2). Almost all of the nucleotide sequences contained the consensus sequences (5′-G-AUCAG-C-GAG-3′), which were positioned at various locations. Interestingly, this consensus sequence was not found in the RNA sequences of pY-binding RNP obtained from the RNP library with randomized 30 nucleotides.[19]

Characterization of the GpYSR-Binding RNP Receptor. Two RNA clones dominated in the 12th round pool, RNA19 and RNA20, were transcribed from the respective DNA sequences, and tested for the GpYSR-binding activity in the presence of

(20) (a) Tong, X.; Drapkin, R.; Yalamanchili, R.; Mosialos, G.; Kieff, E. *Mol. Cell. Biol.* **1995**, *15*, 4735–4744. (b) Yang, J.; Aittomaeki, S.; Pesu, M.; Carter, K.; Saarinen, J.; Kalkkinen, N.; Kieff, E.; Silvennoinen, O. *EMBO J.* **2002**, *21*, 4950–4958.

(21) (a) Jiang, F.; Kumar, R. A.; Jones, R. A.; Patel, D. J. *Nature* **1996**, *382*, 183–186. (b) Fan, P.; Suri, A. K.; Fiala, R.; Live, D.; Patel, D. J. *J. Mol. Biol.* **1996**, *258*, 480–500. (c) Dieckmann, T.; Suzuki, E.; Nakamura, G. K.; Feigon, J. *RNA* **1996**, *2*, 628–640. (d) Dieckmann, T.; Butcher, S. E.; Sassanfar, M.; Szostak, J. W.; Feigon, J. *J. Mol. Biol.* **1997**, *273*, 467–478. (e) Jiang, L.; Patel, D. J. *Nat. Struct. Biol.* **1998**, *5*, 769–774.
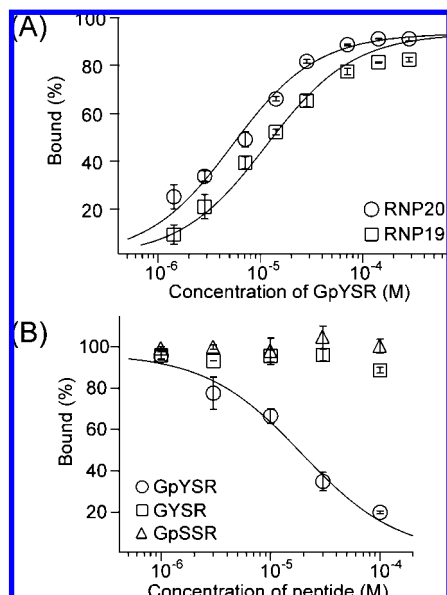
Figure 3. (A) Saturation curves for the binding of RNP19 (open squares) and RNP20 (open circles) to immobilized GpYSR. The fraction of RNP specifically eluted as a function of immobilized GpYSR concentration was plotted and fitted as described in Materials and Methods. (B) Competition binding assays of the GpYSR complex of RNP20 with GpYSR, GYSR, or GpSSR indicate the selective binding of RNP20 to the GpYSR peptide. Binding reactions were performed in the presence of 1 μM RNP20, 1 μL volume of GpYSR agarose resin, and 1 to 100 μM of GpYSR (open circles), GYSR (open squares), and GpSSR (open triangles).

the Rev peptide. Figure 3A shows saturation curves of RNA19/Rev RNP (RNP19) and RNA20/Rev RNP (RNP20) complexes to the immobilized GpYSR peptide. Dissociation constants (K_D) of RNP19 and RNP20 to the GpYSR peptide were determined to be 10 and 4.8 μM, respectively. Both RNP19 and RNP20 showed much higher affinity than those of previously obtained pY-binding RNP receptors (376 μM to 1.4 mM).[19]

Selectivity of RNP receptors for the GpYSR peptide was investigated by competitive binding assays of RNP20. Two GpYSR-derived peptides, a nonphosphorylated peptide Ac-Gly-Tyr-Ser-Arg-NH$_2$ (GYSR) and a peptide containing a phosphorylated serine residue (pS), Ac-Gly-pSer-Ser-Arg-NH$_2$ (GpSSR), were utilized as competitors. RNP20 preferentially bound GpYSR over other GpYSR-derived peptides, GYSR and GpSSR (Figure 3B), indicating that RNP20 possessed a high selectivity for the phosphorylated tyrosine residue. The phosphate groups as well as the aromatic ring of the phosphorylated tyrosine residues were key determinants for the selective binding of RNP20.

Construction of Fluorescent Phosphotyrosine Sensors. GpYSR-binding RNP receptors obtained by in vitro selection were converted to fluorescent sensors according to the method previously reported for the conversion of ATP-binding RNP receptors to fluorescent ATP sensors.[17] The Rev peptide of GpYSR-binding RNP receptors was replaced by a series of fluorophore-labeled Rev peptides to afford various fluorescent GpYSR-binding RNP receptors.

Fluorescent RNP receptors for the GpYSR peptide were constructed by using 13 different RNAs listed in Figure 2, and Rev peptides modified with 4 different fluorophores, 5-carboxy-fluorescein N-succinimidyl ester (5FAM-Rev), 7-methoxycoumarin-3-carboxylic acid (7mC-Rev), 1-pyrenesulfonyl chloride (Pyr-Rev) and Cy5 mono NHS ester (Cy5-Rev), at the N-terminal. Each fluorophore labeled Rev and RNA complex was

placed individually on a multiwell plate, and was evaluated by the change of fluorescence intensities in the absence or presence (1 mM) of the GpYSR peptide by using a microplate reader. Relative ratios of fluorescence intensity (I/I_0) in the absence (I_0) and the presence (I) of GpYSR for fluorescent RNPs with 7mC-Rev, Pyr-Rev, 5FAM-Rev, and Cy5-Rev monitored at 390, 390, 535, and 670 nm, respectively, were summarized in Figure 4A. As with the case for ATP-binding RNP, combination of the RNA subunit pool of the GpYSR-binding RNP and fluorophore-labeled Rev peptides gave combinatorial fluorescent RNP receptor libraries. A number of fluorescent GpYSR sensors emitting from 390 to 670 nm with excitation wavelengths ranging from 355 to 650 nm were obtained from the libraries.

Among the fluorescent RNP20 complexes, RNA20/5FAM-Rev complex showed the highest I/I_0 ratio (Figure 4A). Binding and fluorescent characteristics of RNA20/5FAM-Rev, designated as FRNP20, were investigated in detail. Figure 4B shows the fluorescence spectral changes of FRNP20 upon titration by the free GpYSR peptide. The intensity of fluorescence spectrum around 535 nm increased hyperbolically up to 1.5-fold with the addition of GpYSR peptide. A nonlinear regression analysis of the titration curve yielded a dissociation constant of 4.0 μM for the binding complex of FRNP20 and the GpYSR peptide (Figure 4C), which was in agreement with that of the parent RNP20 and the GpYSR peptide (K_D = 4.8 μM). The specific binding complex formation of FRNP20 was not perturbed by the modification of the Rev peptide in RNP20 with 5FAM at the N-terminal. The environmental perturbation could alter the fluorescence intensity of the fluorophore, possibly due to the conformational changes at the RNA subunit upon binding of GpYSR.

Selectivity of the Fluorescent Phosphotyrosine Sensor. Selective fluorescent sensing of FRNP20 was next analyzed to ask whether FRNP20 retained the ligand-binding selectivity of the parent RNP20 receptor or not. A significant change in the fluorescence intensity of FRNP20 was elicited only by GpYSR, not by the peptides structurally related to GpYSR, such as GYSR or GpSSR (Figure 4C), indicating that the specificity of FRNP20 to GpYSR was parallel to that of the parent RNP receptor (Figure 3B). It is noteworthy to mention that the fluorescence intensity of FRNP20 progressively increased as a function of the concentration of phosphorylated tyrosine within the GpYSR sequence (Figure 4C). Relative fluorescence intensities changed from 1.1 to 1.5 as the concentration of GpYSR increased from 1 to 100 μM. The result indicates that FRNP20 could quantify the amount of phosphorylated peptide GpYSR by fluorescence changes.

The amino acid sequence GYSR corresponds to one of the tyrosine phosphorylation sites, Y88 (EYGM) and Y883 (GYSR), of p100 coactivator. In order to assess whether FRNP20 could discriminate the Y883 site from the other P-site Y88 within the same protein, selective fluorescent sensing of FRNP20 was tested by a tyrosine-phosphorylated peptide EpYGM corresponding to the Y88 site. Titration of FRNP20 with EpYGM revealed a dissociation constant of 380 μM for the FRNP20/EpYGM complex, which had a 95-fold lower affinity as compared to that of GpYSR (Table 1).

(22) Donnelly, R. P.; Dickensheets, H. F.; Finbloom, D. S. *J. Interferon Cytokine Res.* **1999**, *6*, 563–573.
(23) Valiquette, M.; Parent, S.; Loisel, T. P.; Bouvier, M. *EMBO J.* **1995**, *14*, 5542–5549.
(24) Geer, P. V. D.; Hunter, T. *Mol. Cell. Biol.* **1990**, *10*, 2991–3002.
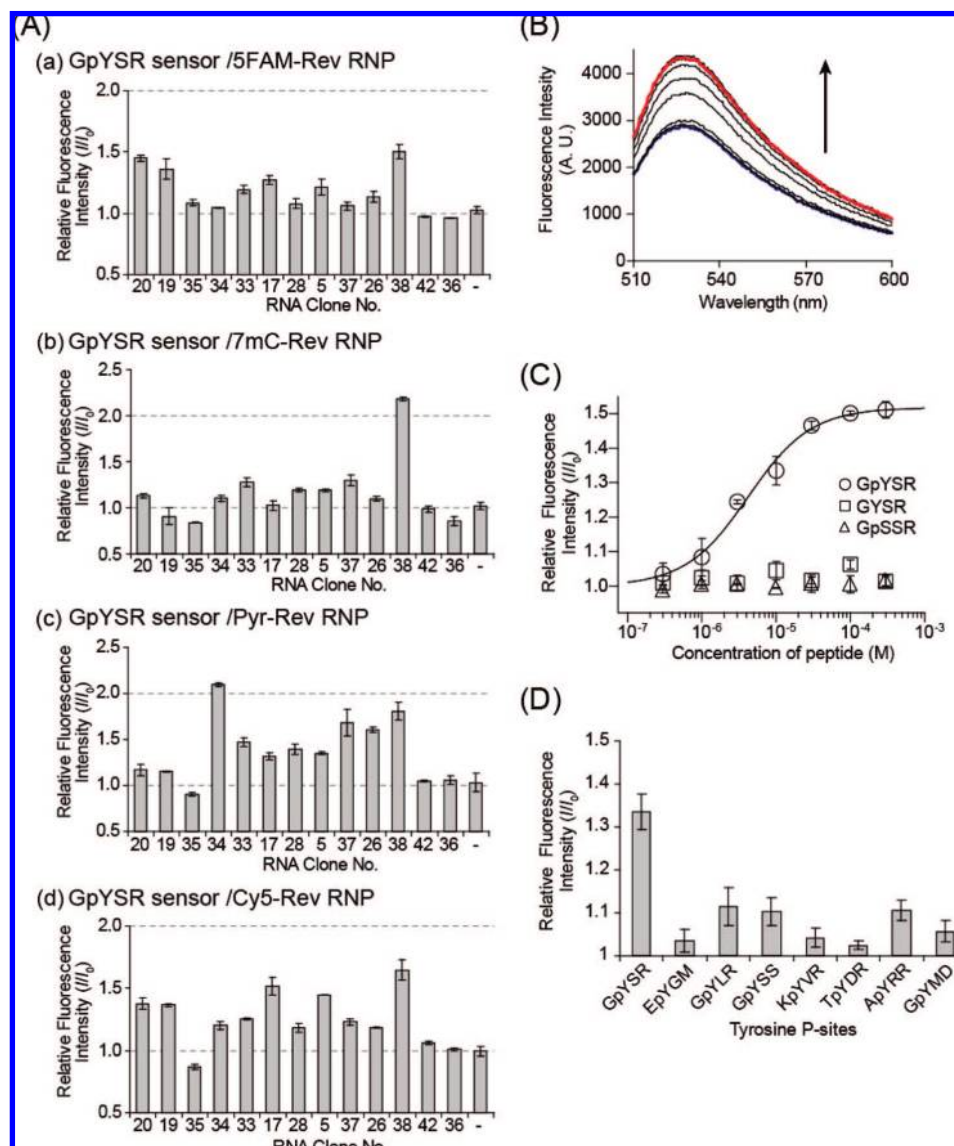
Figure 4. (A) Relative fluorescence intensity changes (I/I_0) of fluorophore-modified RNPs upon GpYSR binding are shown in the bar graphs for (a) 5FAM-Rev RNP, (b) 7mC-Rev RNP, (c) Pyr-Rev RNP, and (d) Cy5-Rev RNP. Relative ratios of fluorescence intensity (I/I_0) were obtained from the fluorescence intensities of the fluorophore-modified RNP in the absence (I_0) and the presence (I) of the GpYSR peptide (1 mM). RNA clones (–) indicate samples without RNA. (B) Direct titration of a fluorescent RNP complex FRNP20 (0.5 μM) with GpYSR (0, 0.3, 1, 3, 10, 30, 100, 300 and 1000 μM) shows an increase in the fluorescence intensity of FRNP20. A spectrum in the absence of GpYSR is shown in blue and in 1000 μM GpYSR in red. (C) Saturation curves for the fluorescence emission intensity of FRNP20 to GpYSR (open circles), GYSR (open squares) or GpSSR (open triangles) indicate FRNP20 responds selectively to the addition of GpYSR. (D) Relative fluorescence intensity changes (I/I_0) of FRNP20 in the presence of various tyrosine-phosphorylated peptides (10 μM) indicate a specific fluorescent response of FRNP20 to the target tyrosine-phosphorylation site.

Selective sensing of the fluorescent RNP sensor FRNP20 was further challenged by the actual phosphorylated tyrosine-containing tetra-amino-acid-sequences reported for native proteins. Relative fluorescence intensity changes of FRNP20 in the presence of various tyrosine-phosphorylated peptides (Figure 4D) clearly demonstrated that the sensor FRNP20 showed a fluorescence response almost exclusively to the target GpYSR peptide. Fluorescent titrations of FRNP20 by the addition of

(25) Ikeda, K.; Wang, L. H.; Torres, R.; Zhao, H.; Olaso, E.; Eng, F. J.; Labrador, P.; Klein, R.; Lovett, D.; Yancopoulos, G. D.; Friedman, S. L.; Lin, H. C. *J. Biol. Chem.* **2002**, *277*, 19206–19212.
(26) Nakazawa, T.; Komai, S.; Tezuka, T.; Hisatsune, C.; Umemori, H.; Semba, K.; Mishina, M.; Manabe, T.; Yamamoto, T. *J. Biol. Chem.* **2001**, *276*, 693–699.
(27) Yokote, K.; Mori, S.; Hansen, K.; McGlades, J.; Pawson, T.; Heldin, C. H.; Claesson-Welsh, L. *J. Biol. Chem.* **1994**, *269*, 15337–15343.
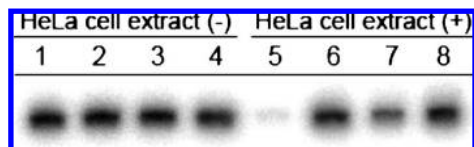
Table 1. Dissociation Constants (K_D) of the FRNP20 Fluorescence Sensor for Phosphorylated Tyrosine-Containing Peptides Derived from Natural Proteins

tyrosine P-sites	kinase	proteins	K_D (μM)
GpYSR	unknown	p100 coactivator[5]	4.0
EpYGM	unknown	P100 coactivator[5]	3.8×10^2
GpY*LR*	Tyk-2	IL-10R1[22]	55
GpYS*S*	InsR	β2AR[23]	68
*K*pY*V*R	Auto	CSF-1 receptor[24]	3.3×10^2
*T*pY*D*R	c-Src	DDR2[25]	1.2×10^2
*A*pY*R*R	Fyn	GluRϵ2[26]	50
GpY*MD*	Auto	PDGF β-receptor[27]	2.4×10^2

the six kinds of tyrosine P-sites derived from natural proteins possessing sequences similar to GpYSR confirmed that the complex of FRNP20 and the GpYSR peptide was the most stable one. Dissociation constants for the complexes with

Figure 5. Stability of FRNP20 in cellular extracts. 5′-^{32}P-labeled RNA20 was incubated in the absence (lanes 1 to 4) or presence (lanes 5 to 8) of HeLa cell extracts for 30 min on ice with RNase inhibitor (lanes 2, 4, 6, and 8) with (lanes 3, 4, 7, and 8) or without (lanes 1, 2, 5, and 6) the 5FAM-Rev peptide. After incubation for 30 min on ice, the labeled RNA were extracted with phenol/chloroform, and then recovered by ethanol precipitation. The recovered samples were separated by 8% PAGE in 6 M urea, and visualized by phosphorimager analysis.

tyrosine-phosphorylated peptides were listed in Table 1. With GpY*L*R, even a single amino acid substitution at the C-terminal to the target pY residue (Ser to Leu) resulted a 14-fold reduction in the affinity of FRNP20. Likewise, a single mutation of Arg to Ser, in GpYS*S* caused a 17-fold reduction in the affinity. Binding of FRNP20 to the *K*pY*V*R peptide indicated that double mutations, Gly to Lys and Ser to Val, caused a 83-fold reduction in affinity. Double mutations of Gly to Thr and Ser to Asp in *T*pY*D*R, and Gly to Ala and Ser to Arg in *A*pY*R*R revealed 31-fold and 13-fold decreases in the affinity, respectively. In addition, double mutations of Ser to Met and Arg to Asp (GpY*MD*) resulted in a 60-fold decrease in the affinity. Thus, FRNP20 showed high specificity to the target GpYSR peptide over other similar tetra-amino-acids peptides corresponding to the native protein tyrosine-phosphorylation sites.

The selectivity of FRNP20 for the amino acid residues adjacent to the phosphorylated tyrosine residue is determined by positively and negatively charged residues, hydrophobic residues, respectively. Comparison of the affinities of the parent GpYSR peptide and GpYS*S* indicates that the Arg residue locating two residues away to the C-terminal from the pY residue contributes to the specific binding of FRNP20. Likewise, the reduced binding affinity of FRNP20 to GpY*L*R and *K*pY*V*R indicates that both Gly and Ser residues locating next to pY are the specificity determinants. These results clearly demonstrated that FRNP20 optically senses not only the phosphorylated tyrosine residue, but also its surrounding three amino acid residues. Reconstitution of the GpYSR-binding RNP receptor RNP20 with a fluorophore-labeled Rev peptide simply and effectively converts GpYSR receptors into fluorescent GpYSR sensors without diminishing the affinity and selectivity of the parent GpYSR receptors (Figure S2 and Table S2 of the Supporting Information).

Detection of the Specific Phosphorylated Tyrosine Residue in Cell Extracts. Finally, fluorescent response of FRNP20 to the GpYSR sequence was tested in HeLa cell extracts. To measure the stability of FRNP20 in cell extracts, 5′-^{32}P-labeled RNA20 was complexed with 5FAM-Rev, which was then incubated in HeLa cell extracts in the presence or absence of RNase inhibitor. After 30 min, RNA was extracted, analyzed by 8% PAGE containing 6 M urea, and visualized by phosphorimager analysis (Figure 5). In the absence of HeLa cell extracts, no degradation of RNA20 was observed in the free form or in the 5FAM-Rev complexed form FRNP20 (Figure 5, lanes 1 to 4). In contrast, free RNA20 was completely degradated in the presence of HeLa cell extracts (Figure 5, lane 5). Upon addition of RNase inhibitor, both free RNA20 and FRNP20 remained predominantly intact in the presence of HeLa cell extracts (Figure 5, lanes 6 and 8). Interestingly, FRNP20 showed significant stability as compared to the free RNA20 in

HeLa cell extracts even in the absence of RNase inhibitor (Figure 5, lanes 5 and 7). Formation of the RNP complex certainly increased the stability of the RNA subunit to nucleases in whole-cell extracts.

A series of samples that contained tyrosine-phosphorylated or nonphosphorylated GpYSR and EpYGM peptides were prepared to represent a mono- or dityrosine-phosphorylated status of p100 coactivator in the HeLa cell extracts. In the presence of GpYSR and EYGM peptides, which represented the status of tyrosine-phosphorylation of p100 coactivator only at Y883, FRNP20 showed a distinct fluorescent response as shown in Figure 6A. As expected, no fluorescent response of FRNP20 was observed upon addition of the GYSR and EYGM peptides (Figure 6B). In the presence of GYSR and EpYGM peptides, which represented the status of tyrosine-phosphorylation of p100 coactivator only at Y88, FRNP20 showed no fluorescent response (Figure 6C). When both of the peptides GpYSR and EpYGM were phosphorylated (Figure 6D), FRNP20 revealed a fluorescent response almost equal to that observed in the presence of GpYSR and EYGM peptides (Figure 6A). These results indicated that FRNP20 has a potential to discriminate the unique pY-containing amino-acid sequence even in cell extracts.

Conclusions

The fluorescent RNP sensors for the phosphotyrosine-containing GpYSR peptide represent the first example of the RNA aptamer-based artificial receptor for the phosphotyrosine-containing tetra-amino-acid motif. The combinatorial strategy using the modular RNP receptor enables efficient tailoring of a novel fluorescent sensor for a specific phosphorylated tyrosine residue within a defined tetra-amino-acid motif. The pY sensor for the phosphorylated tyrosine residue enabled selective monitoring of a specifically phosphorylated tyrosine residue within GpYSR by fluorescent responses even in the presence of the other phosphorylated tyrosine residue. In addition, the pY sensor FRNP20 specifically responded to the phosphorylated tyrosine residue within the target amino acid sequence in HeLa cell extracts. These results indicate potential applications of the RNP-based fluorescent phosphotyrosine sensor for mapping phosphorylated-tyrosine-related signaling pathways. Although the affinity of the pY sensor reported here is not high enough for practical use, it would be possible to obtain RNP receptors or RNP sensors with higher affinity by using larger phosphorylated peptide fragments or phosphorylated proteins. In fact, RNA aptamers with dissociation constants less than a nanomolar range has been isolated by using whole proteins.[28] Systematic construction of fluorescent RNP sensors for the pY residues within defined amino-acid sequences would provide a new proteomics methodology that accelerate assessment of specific post-translational modification of proteins to provide a more detailed view of cellular signal transductions.

Materials and Methods

Materials. *N*-α-Fmoc-protected amino acids, HBTU (2-(1H-benzotriazole-1-yl)-1,1,3,3-tetramethyl uronium hexafluorophosphate), 1-hydroxybenzotriazole (HOBt), DIEA (*N*, *N*-diisopropylethyl amine), TFA (trifluoroacetic acid), and distilled DMF (*N*, *N*-dimethylformamide) were obtained from Watanabe Chemical Industry. Fmoc-PAL-PEG resin (0.38 mmol/g) was purchased from Applied Biosystems. Solid phase peptide synthesis was carried out by a peptide synthesizer PSSM-8 (Shimadzu). HPLC grade acetonitrile (Nacalai tesque) was used for both analytical and preparative HPLC. A reversed-phase C18 column (20 × 250 mm, Ultron VX-
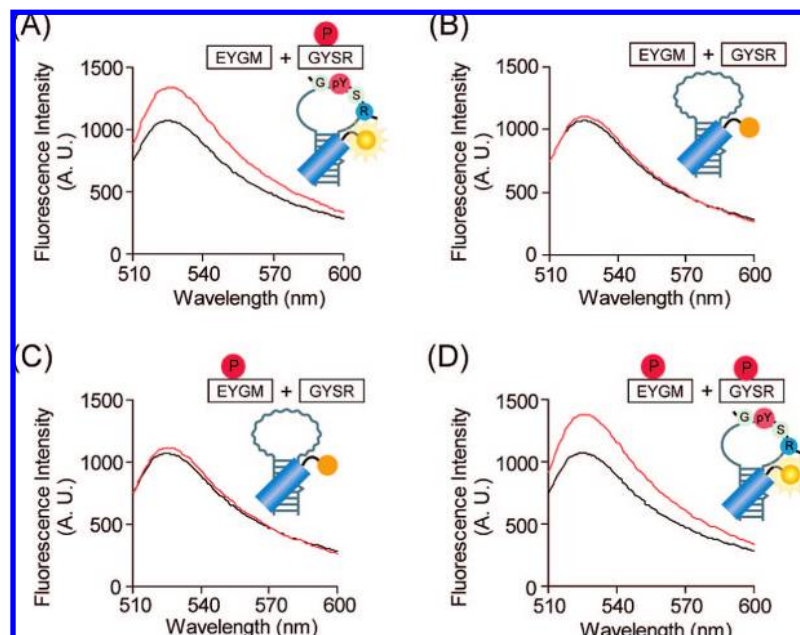
Figure 6. Fluorescence spectra of FRNP20 in HeLa cell extracts in the abesence (black lines) and in the presence of peptides (A) EYGM and GpYSR, (B) EYGM and GYSR, (C) EpYGM and GYSR, and (D) EpYGM and GpYSR (red lines) indicate that FRNP20 responds specifically to the tyrosine-phosphorylation at the GpYSR site, not to the EpYGM site of coactivator p100. Each sample (300 μL) contained 0.5 μM FRNP20, 5 μM peptide, RNasin (1 unit/μL), Halt Phosphatase Inhibitor Cocktail (10 μL/mL), and HeLa cell extracts (protein concentrations 1.88 mg/mL).

Peptide, Shinwa Chemical Industry) and a RESOURCE-RPC column (3 mL, Pharmacia) were used for purification of peptides for preparative purpose. Analytical HPLC were carried out on a reversed-phase C18 column (4.6 × 150 mm, Ultron VX-Peptide, Shinwa Chemical Industry). The products were confirmed using a MALDI-TOF mass spectrometer Voyager DE-STR (PerSeptive Biosystems) and an NMR spectrometer JNM-ECP300 (JEOL). NHS-activated Sepharose 4 Fast Flow (immobilized on cross-linked 4% beaded agarose, 16−23 μmol NHS/mL) was purchased from Pharmacia Biotech. T4 polynucleotide kinase was purchased from New England Biolab. [γ-^{32}P]adenosine-5′-triphosphate was purchased from Amersham. Dulbecco's modified Eagle's medium (DMEM) was purchased from Sigma-Aldrich. Trypsine was purchased from Gibco. Streptomycin was purchased from Meiji Seika. Gel electrophoresis grade acrylamide, bisacrylamide, and Fetal Bovine Serum (FBS) were obtained from Wako Chemicals. All other chemicals were reagent grade and used without further purification. Rev peptide modified with 5-carboxyfluorescein *N*-succinimidyl ester (5FAM-Rev), 7-methoxycoumarin-3-carboxylic acid (7mC-Rev), 1-pyrenesulfonyl chloride (Pyr-Rev), and Cy5 mono NHS ester (Cy5-Rev) were synthesized as described previously.[17]

Synthesis of Tetrapeptides Containing Phosphotyrosine. Tetrapeptides containing phosphotyrosine, tyrosine, or phosphoserine were synthesized according to the Fmoc chemistry protocols by using Fmoc-PAL-PEG resin, *N*-α-Fmoc-protected amino acid and HBTU. The peptide was cleaved from the resin and deprotected by phenol (0.75 g), distilled water (0.5 mL), thioanisol (0.5 mL), 1,2-ethanditiol (0.25 mL), and TFA (10 mL) depending on the nature of protecting groups. Deprotected peptides were purified by a reversed-phase HPLC. The *C*-terminal of peptides were amidated, and the *N*-terminal of peptides were acetylated. Peptide concentrations were determined using phosphotyrosine absorbance with λ_{267} = 500 M^{-1}cm^{-1} and tyrosine absorbance with λ_{274} = 1420 M^{-1}cm^{-1}.

GpYSR. (Ac-Gly-pTyr-Ser-Arg-NH$_2$) ^{1}H NMR (300 MHz, D$_2$O): δ1.05−1.32 (*m*, 4 H), 1.50 (*s*, 3 H), 2.39−2.69 (*m*, 4 H), 3.20−3.35 (*m*, 4 H), 3.73 (*m*, 1 H), 3.85 (*m*, 1 H), 4.06 (*m*, 1 H), 6.57 (*d*, *J* = 8.5 Hz, 2 H), 6.65 (*d*, *J* = 8.5 Hz, 2 H); TOF-mass: [M+H]$^+$ calcd. 603.54, found 603.78.

GYSR. (Ac-Gly-Tyr-Ser-Arg-NH$_2$) ^{1}H NMR (300 MHz, D$_2$O): δ1.62−2.00 (*m*, 4 H), 2.03 (*s*, 3 H), 2.95−3.13 (*m*, 2 H), 3.24 (*m*, 2 H), 3.79−3.97 (*m*, 4 H), 4.33 (*m*, 1 H), 4.39 (*m*, 1 H), 4.62 (*m*, 1 H), 6.87 (*d*, *J* = 8.2 Hz, 2 H), 7.15 (*d*, *J* = 8.2 Hz, 2 H); TOF-mass: [M+H]$^+$ calcd. 523.56, found 523.83.

GpSSR. (Ac-Gly-pSer-Ser-Arg-NH$_2$) ^{1}H NMR (300 MHz, D$_2$O): δ1.58−2.03 (*m*, 4 H), 2.08 (*s*, 3 H), 3.23 (*m*, 2 H), 3.86−4.07 (*m*, 4 H), 4.15−4.38 (*m*, 3 H), 4.49 (*m*, 1 H), 4.65 (*m*, 1 H); TOF-mass: [M+H]$^+$ calcd. 527.45, found 527.84.

EpYGM. (Ac-Glu-pTyr-Gly-Met-NH$_2$) ^{1}H NMR (300 MHz, D$_2$O): δ1.75−2.17 (*m*, 10 H), 2.22−2.40 (*m*, 2 H), 2.43−2.64 (*m*, 2 H), 2.94−3.01 (*m*, 1 H), 3.11−3.18 (*m*, 1 H), 3.77−3.94 (*m*, 2 H), 4.23 (*m*, 1 H), 4.44 (*m*, 1 H), 4.56 (*m*, 1 H), 7.10 (*d*, *J* = 8.4 Hz, 2 H), 7.19 (*d*, *J* = 8.2 Hz, 2 H); TOF-mass: [M+Na]$^+$ calcd. 642.57, found 642.96.

KpYVR. (Ac-Lys-pTyr-Val-Arg-NH$_2$) ^{1}H NMR (300 MHz, D$_2$O): δ0.88 (*m*, 6 H), 1.25 (*m*, 2 H), 1.58−1.81 (*m*, 8 H), 1.99 (*m*, 4 H), 2.88−3.07 (*m*, 4 H), 3.22 (*m*, 2 H), 4.00 (*m*, 1 H), 4.12−4.25 (*m*, 2 H), 7.09 (*d*, *J* = 8.5 Hz, 2 H), 7.17 (*d*, *J* = 8.2 Hz, 2 H); TOF-mass: [M+H]$^+$ calcd. 686.72, found 686.85.

TpYDR. (Ac-Thr-pTyr-Asp-Arg-NH$_2$) ^{1}H NMR (300 MHz, D$_2$O): δ1.05−1.17 (*m*, 3 H), 1.51−1.92 (*m*, 4 H), 2.04 (*s*, 3 H), 2.73 (*m*, 1 H), 2.89 (*m*, 1 H), 3.03 (*m*, 2 H), 3.17 (*m*, 2 H), 4.08 (*m*, 1 H), 4.22 (*m*, 2 H), 4.60 (*m*, 2 H), 7.09 (*d*, *J* = 8.5 Hz, 2 H), 7.17 (*d*, *J* = 8.5 Hz, 2 H); TOF-mass: [M+H]$^+$ calcd. 675.61, found 675.87.

GpYLR. (Ac-Gly-pTyr-Leu-Arg-NH$_2$) ^{1}H NMR (300 MHz, D$_2$O): δ0.87−0.94 (*m*, 6 H), 1.57−1.88 (*m*, 7 H), 2.05 (*s*, 3 H), 3.07 (*m*, 2 H), 3.23 (*m*, 2 H), 3.87 (*m*, 2 H), 4.25−4.36 (*m*, 2 H), 4.62 (*m*, 1 H), 7.14 (*d*, *J* = 8.7 Hz, 2 H), 7.20 (*d*, *J* = 8.2 Hz, 2 H); TOF-mass: [M+H]$^+$ calcd. 629.62, found 629.59.

ApYRR. (Ac-Ala-pTyr-Arg-Arg-NH$_2$) ^{1}H NMR (300 MHz, D$_2$O): δ1.32 (*d*, *J* = 7.1 Hz, 3 H), 1.46−1.93 (*m*, 8 H), 2.08 (*s*, 3 H), 3.01−3.27 (*m*, 6 H), 4.24 (*m*, 3 H), 4.57 (*m*, 1 H), 7.14 (*d*, *J* = 8.2 Hz, 2 H), 7.21 (*d*, *J* = 8.2 Hz, 2 H); TOF-mass: [M+H]$^+$ calcd. 686.68, found 686.66.

GpYMD. (Ac-Gly-pTyr-Met-Asp-NH$_2$) ^{1}H NMR (300 MHz, D$_2$O): δ1.86−2.05 (*m*, 8 H), 2.35−2.54 (*m*, 2 H), 2.76−3.12 (*m*, 4 H), 3.84 (*m*, 2 H), 4.39 (*m*, 1 H), 4.55 (*m*, 1 H), 4.65 (*m*, 1 H),

7.11 (*d*, *J* = 7.6 Hz, 2 H), 7.18 (*d*, *J* = 7.4 Hz, 2 H); TOF-mass: [M+Na]$^+$ calcd. 628.55, found 628.80.

GpYSS. (Ac-Gly-pTyr-Ser-Ser-NH$_2$) ^{1}H NMR (300 MHz, D$_2$O): δ 1.99 (*s*, 3 H), 2.98−3.17 (*m*, 2 H), 3.77−3.95 (*m*, 6 H), 4.40−4.87 (*m*, 2 H), 4.65 (*m*, 1 H), 7.13 (*d*, *J* = 8.5 Hz, 2 H), 7.22 (*d*, *J* = 8.5 Hz, 2 H); TOF-mass: [M+Na]$^+$ calcd. 556.42, found 556.91.

Abbreviations for the amino acid are as follows: A, Ala; D, Asp; E, Glu; G, Gly; K, Lys; L, Leu; M, Met; R, Arg; S, Ser; T, Thr; Y, Tyr; pY, phosphotyrosine; pS, phosphoserine.

GpYSR Agarose Resin Preparations. NHS-activated Sepharose 4 Fast Flow was handled according to manufacture's instructions. H-Gly-pTyr-Ser-Arg-NH$_2$ (10 mM, 7.5 mL) or H-Gly-pTyr-Ser-Arg-NH$_2$ (20 μM, 7.5 mL) were incubated with NHS-activated Sepharose 4 Fast Flow (the volume of 5 mL) overnight at 4 °C with mild rotation, followed by washing. Afterward, the GpYSR-modified agarose resins were resuspended and stored in 20% ethanol (50 mL) at 4 °C. Quantitation of the immobilized ligands were determined by Briggs phosphate test.[29]

Nucleic Acids Preparations. The original double-stranded DNA pools were constructed by Klenow polymerase (New England Biolabs) reaction from a synthesized oligonucleotide containing 40 random nucleotides [5′-GGAATAGGTCTGGGCGCA-N$_{40}$-P(OH)-3′] and a synthesized oligonucleotide containing 7 random nucleotides (5′-GGAATAGGCCTGTACCGTCA-N$_7$-OH-3′) followed by PCR amplification to add the promoter for T7 RNA polymerase using Pyrobest DNA polymerase (TaKaRa) with 3′-DNA (5′-GGAATAG-GCCTGTACCGTC-3′) and 5′-DNA primer (5′-TC<u>TAATACGACT-CACTATAG</u>GAATAGGTCTGGGCGCA-3′: T7 RNA promoter is underlined). RNA transcription was performed using an AmpliScribeT7 kit (Epicenter) for 3 h at 37 °C, according to the supplier's recommended protocols. The resulting RNA was phenol/chloroform extracted, precipitated with ethanol, and pelleted by centrifugation. The RNA was purified by denaturing polyacrylamide gel electrophoresis and eluted. Concentrations of RNAs were determined by UV spectroscopy.

In Vitro Selection Procedures. RNPs that bound GpYSR were selected as follows: RNA was heated at 80 °C for 3 min and chilled for proper secondary structure. In the first to third rounds of selection, a binding buffer [50 μL, 10 mM Tris-HCl (pH 7.6), 100 mM KCl, 10 mM MgCl$_2$, 0.005% Tween20] containing 2 μM RNA, 3 μM Rev and 20 μL volume of GpYSR agarose resin (9.2 μmol/mL, determined by Briggs phosphate test[29]) was incubated to allow the formation of a specific ribonucleopeptide complex for 30 min on ice, with the exception of the selection from the fourth to sixth rounds, an RNP pool with 2 μL volume of GpYSR agarose resin (9.2 μmol/mL), and from the seventh to twelfth rounds, an RNP pool with 20 μL volume of GpYSR agarose resin (2.7 nmol/mL, determined by Briggs phosphate test[29]). RNP/GpYSR resin complexes were washed 3× with 300 μL of binding buffer to remove unbound RNPs and eluted three times with 100 μL of binding buffer containing 0.2 mM H-Gly-pTyr-Ser-Arg-NH$_2$. Recovered RNPs were precipitated with ethanol and resuspended in TE buffer. After reverse transcription with AMV reverse transcriptase (Promega) of the selected RNA using the 3′-DNA primer used in PCR amplification and successive PCR amplification (RT-PCR) using the 5′- and 3′-DNA primers, the DNA templates were transcribed, and the resulting RNAs were subjected to the next round of selection. Selected RNA pools were converted to DNA and PCR-amplified to introduce *Bam*HI, *Eco*RI restriction sites by using primers 5′-GCGGGATCCTTTCGGCCTGTACCGTCA-3′ and 5′-CGGAATTCTAATACGACTCACTATAGG-3′. After enzymatic digestion (New England Biolabs), DNAs were cloned into the pUC19 vector using Ligation Kit Ver. Two (TaKaRa) and sequenced using a BigDyeTerminator Cycle Sequencing Kit (Applied Biosystems) with a model 377 DNA sequencer and 3130/3130×l genetic analyzer (Applied Biosystems).

Quantitation of the Immobilized Ligand: Measurements by Using an Immobilized GpYSR Resin. The affinity of the ribonucleopeptide complexes for GpYSR was determined by measuring the fraction of ribonucleopeptide bound to GpYSR agarose resin at a range of immobilized ligand concentrations in a binding buffer containing 10 mM Tris-HCl (pH 7.6), 10 mM KCl, 20 mM MgCl$_2$, and 0.005% Tween20. The concentration of GpYSR available for binding was determined by saturating GpYSR agarose resin with excess amounts of ^{32}P end-labeled the RNA20/Rev complex for GpYSR and measuring the amount of RNA20/Rev specifically eluted upon elution buffer containing 10 mM Tris-HCl (pH 7.6), 10 mM KCl, 20 mM MgCl$_2$, 0.005% Tween20 and 2 mM GpYSR. The available GpYSR concentration on the GpYSR agarose resin was estimated at 142 nmol/mL by assuming that a single ribonucleopeptide bound per GpYSR molecule. For binding studies, an RNA20/Rev with 2 μL volume of GpYSR agarose resin (1.1 nmol/mL, determined by Briggs phosphate test[29]). RNP20/GpYSR complexes were washed with 400 μL of binding buffer to remove unbound RNPs and eluted 2× with 150 μL of binding buffer containing 2 mM Ac-Gly-pTyr-Ser-Arg-NH$_2$. The fractions of RNA bound to the GpYSR agarose resin were quantitated by Cherenkov counting in a scintillation counter. The fraction of ribonucleopeptide specifically eluted as a function of immobilized GpYSR concentration was plotted and fitted by nonlinear regression to the equation:

$$f = ((([GpYSR] + [RNP] + K_D) - (([GpYSR] + \\ [RNP] + K_D)^2 - (4[GpYSR])[RNP])^{1/2})/2) \quad (1)$$

where *f* is the fraction of input ribonucleopeptide bound to the matrix, K_D is the apparent dissociation constant of ribonucleopeptide for GpYSR.

Ligand-Binding Competition Assay. Double-stranded DNA templates were prepared by PCR amplification from individual clones by using the 5′- and 3′-DNA primers, and these templates were transcribed as described above. Individual RNAs were labeled at the 5′-terminal with T4 Polynucleotide kinas and [γ-^{32}P] ATP. The competition assay was performed as follows: A binding buffer [20 μL, 10 mM Tris-HCl (pH 7.6), 100 mM KCl, 10 mM MgCl$_2$, 0.005% Tween20] containing 1 μM RNA, 1 μM Rev, and 1 μL volume of GpYSR agarose resin (142 nmol/mL) was incubated for 30 min on ice in the presence of competitive ligand. RNP/GpYSR complexes were washed with 400 μL of binding buffer to remove unbound RNPs and eluted 2× with 150 μL of binding buffer containing 0.2 mM Ac-Gly-pTyr-Ser-Arg-NH$_2$. The fractions of RNA bound to the GpYSR agarose resin were quantitated by Cherenkov counting in a scintillation counter (Beckman multipurpose scintillation counter LS6500).

Determination of the Equilibrium Dissociation Constants. The affinity of the RNPs for GpYSR was determined by measuring the fraction of RNP bound to GpYSR agarose resin at a range of ligand concentrations in a binding buffer containing 10 mM Tris-HCl (pH 7.6), 100 mM KCl, 10 mM MgCl$_2$, 0.005% Tween20 as described previously. For competition assay, the fraction of the RNP specifically eluted as a function of immobilized GpYSR concentration was plotted and fitted by nonlinear regression to a function of the form:

$$f = ((K_D + K_D[competitor]/K_D' + [GpYSR] + [RNP] - \\ ((K_D + K_D[competitor]/K_D' + [GpYSR] + [RNP])^2 - \\ (4[GpYSR][RNP]))^{1/2})/(2[RNP])) \quad (2)$$

where *f* is the fraction of bound RNP to input RNP, [RNP] is the concentration of ribonucleopeptide, and K_D is the dissociation constant of RNP/GpYSR agarose resin. K_D' is the dissociation constant of RNP/competitor complex.

Fluorescence Spectral Measurements. Fluorescence spectra were recorded on a Hitachi F-4500 fluorescence spectrofluorophotometer with excitation and emission bandwidth of 5 nm. All measurements were performed at 4 °C in a buffer (250 μL) containing 10 mM Tris-HCl (pH 7.6), 100 mM KCl, 10 mM MgCl$_2$, 0.005% Tween20,

(28) Seiwert, S. D.; Stines Nahreini, T.; Aigner, S.; Ahn, N. G.; Uhlenbeck, O. C. *Chem. Biol.* **2000**, *7*, 833–843.

fluorescent RNP (0.5 μM) and indicated concentration of ligand. Excitation wavelength was 5FAM-Rev (494 nm).

Fluorescence Measurements on the Microplate. The 96-well fluorescence measurements were performed on a Wallac ARVOsx 1420 multilabel counter. A binding solution (100 μL) containing 1 μM of fluorescent RNP in 10 mM Tris-HCl (pH 7.6), 100 mM KCl, 10 mM MgCl$_2$, 0.005% Tween20 with indicated concentration of ligand was gently swirled for a few minutes and allowed to sit for 30 min. Emission spectra were measured with an appropriate filter set for each fluorophore. Excitation and emission wavelengths were 5FAM-Rev (485 nm, 535 nm), Cy5-Rev (650 nm, 670 nm), 7mC-Rev (355 nm, 390 nm) and Pyr-Rev (355 nm, 390 nm).

Determination of Binding Affinity by Fluorescence Titrations. The GpYSR-binding affinity of fluorescent RNP was obtained by fitting the GpYSR titration data using the equation:

$$F_{obs} = A(([\text{FRNP}]_T + [\text{GpYSR}]_T + K_D) - (([\text{FRNP}]_T + [\text{GpYSR}]_T + K_D)^2 - 4[\text{FRNP}]_T[\text{GpYSR}]_T)^{1/2})/2[\text{FRNP}]_T \quad (3)$$

where A is the increase in fluorescence at saturating GpYSR concentrations ($F_{max} - F_{min}$), K_D is the dissociation constant, and [FRNP]$_T$ and [GpYSR]$_T$ are the total concentrations of fluorescent RNP and GpYSR, respectively.

Preparation of HeLa Cell Extracts. HeLa cells were seeded at 3×10^6 cells on a 10 cm diameter dish and cultured in DMEM supplemented with 10% FBS, penicillin (30 units/mL), and streptomycin (30 μg/mL) at 37 °C in a humidified atmosphere consisting of 5% CO$_2$ and 95% air. After a three-day culture, cells were trypsinized and harvested. The pelleted cells were suspended in binding buffer (10 mM Tris-HCl, 100 mM KCl, 10 mM MgCl$_2$, 0.005% Tween20) and sonicated for 12 min to obtain cell lysate.[30]

The homogenate was checked microscopically for cell lyses. The cell lysate was centrifuged at 12000 $\times g$ for 5 min. The supernatant was passed through 0.4 μm filter and measured by RC DC protein assay kit (BioRad). The total protein amount of supernatant was 1.88 mg/mL.

Stability of RNP in HeLa Cell Extracts. A 0.5-μM portion of RNA20 or a 0.5-μM RNA20/5FAM-Rev containing 5′-^{32}P-labeled RNA20 was incubated on ice in binding buffer [100 μL, 10 mM Tris-HCl (pH 7.6), 100 mM KCl, 10 mM MgCl$_2$, 0.005% Tween20] in the presence or absence of 1 unit/μL RNasin (Promega) with or without HeLa cell extracts. Reaction products were extracted 3$\times$ with an equal volume of phenol and chloroform, followed by precipitation with 2.5 volumes of ethanol and 0.1 volumes of 3 M sodium acetate. The recovered samples were separated by 8% PAGE in 6 M urea and visualized by phosphor imager analysis (Amersham Pharmacia).

Supporting Information Available: Characterization of an RNA library RRENn containing the randomized nucleotides with variable lengths adjacent to the RRE region (Figure S1) and results of competitive binding titration assay of the RNP20 complex by using naturally occurring phoshorylated tyrosine-containing peptide (Figure S2 and Table S1). This material is available free of charge via the Internet at http://pubs.asc.org

JA801734F

(29) Sawyer, D. A.; Potter, B. V. L. *J. Chem. Soc., Perkin Trans. 1* **1992**, 923–932.

(30) Endoh, T.; Funabashi, H.; Mie, M.; Kobatake, E. *Anal. Chem.* **2005**, *77*, 4308–4314.